Journal of Advanced Marine Engineering and Technology, Vol. 49, No. 4, pp. 314~323, 2025
J. Advanced Marine Engineering and Technology (JAMET)
https://doi.org/10.5916/jamet.2025.49.4.314

ISSN 2234-7925 (Print)
ISSN 2765-4796 (Online)
Original Paper

Container ship model experiment of autonomous course-keeping ability at the beach

Gi-Seon Jeong[1] · Sang-Do Lee[†]

(Received August 2, 2025 ; Revised August 20, 2025 ; Accepted August 27, 2025)

Abstract: Recently, the autonomous operation of vehicles has drawn great attention. To supplement the limitations of simulation methods and applications to real ships for autonomous navigation, we made a container ship model and tested it autonomously in a coastal sea environment. Our goal is to enhance the course-keeping ability with PD control, which is based on the Pixhawk 4 and QgroundControl. We focus on course track errors, vibrations, and rotational stability of the model at sea. We made a 20,000 TEU container ship model with a single rudder and propeller. A hull was made of fiberglass material for the purposes, such as low weight for the repetitive tests and maintenance, sufficient strength against wave, and inner spaces for the equipment of propulsion and batteries. As a result, the course track errors were recorded with an error of less than 1 m except over 2 m in the edges of a star-shaped route. The bow shape of the model cuts through the sea surface effectively, as evidenced by the vibration in the x-direction that does not exceed 1.5×10^{-9} m/s/s. The roll angles were not exceeded by 10 ° during autonomous course-keeping test. In addition, the constant patterns of trajectories are one of the advantages of USV systems. However, the absence of cargo functionality as well as the bottom-heavy design is a limitation of the ship.

Keywords: Container ship model, Experiments, Course-keeping ability, Ocean environments, USV

1. Introduction

Recently, as the autonomous operation of vehicles has drawn considerable attention, the authors have naturally become interested in an Unmanned Surface Vehicle (USV) of the marine environment. When the author attempted to study the motion stabilization of marine vessels, experiments at sea were one of the remaining tasks to be continued. Then, does the author doubt that the marine vessels can be stabilized according to the control theory? Active control achievements will be upgraded with the addition of the experiment. There was a chance for a small experiment, and so we prepared for the test of a ship model. The starting point of this study was to realize the parametric instability of the admirable M. Faraday **[1]**, we did not fulfill such a goal.

As is well known, the concept of a traditional ship, as well as the role of humans involved in marine vessels, will change according to the emergence of USVs. There are many risks of actual operation, even though the technologies of USVs have been well developed for decades. For the safe operation and economic value of USVs, it is necessary to ponder their emergence. For example, how can we handle the resonance roll of USVs that is not solved even now among the existing container ships in the ocean environment? **[2]** Can the heartbreak of design still attract the interest of owners? Nevertheless, the owners are making the largest container ships year after year **[3]**.

When we think about the USV, why can the hull of modern container ships hardly be seen at the contests of autonomous operation **[4]**? Why are the ocean environments hardly specified in the studies **[2]**? Is the numerical simulation possible in the real seas **[5]**? The goal of our interests in USVs can be summarized as follows:

1) The USV should be tested repeatedly. The costs of experiments in a towing tank are not cheap for an individual researcher **[6]**. The equipment of general USVs is not light enough to move by hand like *ARAGON* **[7]**. The

† Corresponding Author (ORCID: http://orcid.org/0000-0002-7001-4761): Assistant Professor, Division of Navigation & Information System, Mokpo National Maritime University, 91, Haeyangdaehak-ro, Mokpo, Jeollanam-do, 58628, Korea, E-mail: oksangdo@mmu.ac.kr, Tel: 061-240-7257

1 Ph. D. Candidate, Division of Maritime Transport System, Mokpo National Maritime University, E-mail: capitanojkor@hanmail.net, Tel: 061-651-1006

repair should be easily accessible. Constructing such a systematic environment demands large expenses. Thus, the USV systems are difficult to develop personally. So, sometimes we have to use the approaches from the numerical studies. For example, the ocean environments of the simulation field by the CFD (Computational Fluid Dynamics) can be varied **[8]**. It means that the test place seems to be unclear. In addition, the path-following control of USV asks authors whether it is possible in the ocean **[5]**? That's why the authors tried to find this approach.

2) The design of a modern container ship is important to us, even though the trends of USV have changed, of course. There are more advantages than drawbacks to the recent design of container ships. So, we selected the fiberglass for hull strengths of bare necessities against wave **[9]**, inner spaces for batteries and propulsion systems, and geometrical beauty of a container ship.

There are well-known standard models, such as KCS, KVLCC 1 and 2; however, we select the recent trends of a very-large container ship (VLCS) model because there are no publications relating to such a recent model. We followed general characteristics of modern container ships, such as an overhanging transom stern and pronounced bow flare **[2]**.

The path-tracking problem of marine vessels has been solved via sliding mode control **[10]**, model-predictive control **[11]**, reinforcement learning approach **[12]-[14]**, and prescribed performance control **[15]**. Kang and Jung **[16]** similarly studied on automatic operation control of autonomous ships. Influenced by their results, the authors thought that the model, performance, and principles should be improved. In the study, our goal is to enhance the course-keeping ability with PD control, which is based on the Pixhawk 4 and QGroundControl **[17]**, a preferred choice among drone users **[18]**. QGroundControl is one of the open-source programs, such as ArduPilot. Then, we carried out many trials on the coastal sea of Yeosu, South Korea. This study organizes one of the results of the course-keeping experiment based on the VLCS model.

The originality of this study is that the hull of the ship is made by the authors. It is difficult to find publications relating to the recent VLCS model with autonomous testing in the ocean field based on the Pixhawk 4 and QGroundControl. This study does not develop the mathematical skill of control schemes. In addition, the illustration of guidance laws clearly will help readers understand the principles.

2. Experimental setup

2.1 Container Ship Model

In the recent trend of a VLCS, the length overall (LOA) does not make it longer than 399.9 m. Inspired by COSCO Shipping *Gemini* having the length **[19]**, we adjusted the scale ratio of 1/320 based on a 20,000 TEU ship. Considering the portable size, the LOA and beam of our model are selected as 1,250 and 185 mm, respectively. **Table 1** lists the main parameters of the ship model. The draft and hull weights make us anticipate the stability of the roll motions of the model. It is a bottom-flat type and a heavy bottom model. We did not show the hydrodynamic information of this model in detail. It will be the next topic with the numerical simulations. See reference in **[2]**.

At first, we prepared the Iso-pink on the desk (**Figure 1a**). With a saw, we roughly cut the material. Then we carefully polished the Iso-pink (**Figure 1b**). Then it was taped to protect before rubbing the fiberglass (**Figure 1c**).

The fiberglass and synthetic resins are put into the hull (**Figure 2a**). The hull of fiberglass is widely used because of its various merits, such as strength, lightness, low cost, and elasticity. Both the inner space and strength within the portable size make this material recommended. Basic painting with white color and the work of grinding was done several times to smooth the surface

(a) (b) (c)

Figure 1: Model construction process

Table 1: Main parameters of the ship model

Parameters	Value	Unit
LOA	1,250	mm
Breadth	185	mm
Depth	108	mm
Draft (Max)	74	mm
Total weight	11,480	g
Hull weight	8,150	g

of hull (**Figure 2b**). Then, the painting with blue and red colors, which separates the load lines and preserves the preliminary buoyancy by the height of a freeboard, was finished (**Figure 2c**). The maximum draft of the VLCS model should be kept within the boundary of the blue and red colors of the hull. This point should be checked before going out to sea.

(a)

(b)

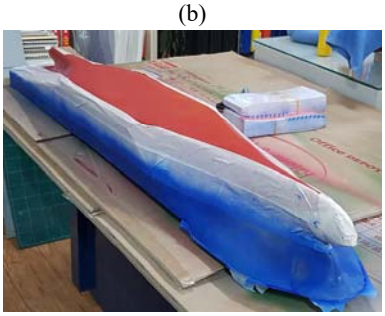

(c)

Figure 2: Hull process of fiberglass and painting

(a)

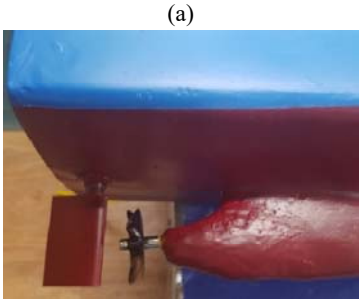

(b)

Figure 3: Snapshots of bow and stern

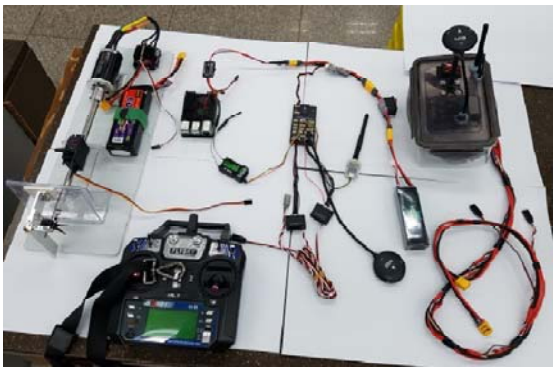

Figure 4: Equipment for an autonomous tracking system

Let's see the form of the bow and stern. The bulbous bow was not fully constructed according to the author's opinion, rather, it seems to be closer to an ax bow. There are tiny holes in the bow thrusters below the VLCS model (**Figure 3a**). The transversal beam of the position of the bow thrusters is not sufficient. Because the thrusters were not so effective, we decided not to use them. How can we balance the ship if we use the different weights of cargo and ballast tanks, except for the propulsion system, in this size of hull space? So, the too small size of the model of USVs may lose the beauty of the ship itself because its purpose is far from transportation and operation in ocean environments. Even though it is not so meaningful, the stern skeg is made as slim as possible against the wave breaking and viscous resistance (**Figure 3b**). The single rudder and propeller can be seen as well. A rubber tube was used to cover the propeller shaft. The long and narrow stern tube should be protected from the inflow of seawater.

Figure 4 shows the equipment of the autonomous tracking system. We arranged the table to announce the simple structures of actuation. We employed various products, including the Holybro Pixhawk 4, Holybro SiK telemetry radio V3, Raspberry Pi 4 Model B, FLYSKY FS-i6 receiver, SeaKing-60A-V3.1 speed controller, 3680-880 KV brushless motors, and a laptop.

Holybro SiK telemetry can work well with Micro Air Vehicle Link (MAVLink) packets and be integrated with the Mission Planner and QGroundControl **[20].** Even if the distance between the model ship and the computer is relatively far, information exchange is possible through two telemetries, which are connected to the Pixhawk 4 and a laptop. There are major sensors, such as GPS, Inertial Measurement Units (IMU), which include accelerometers and gyroscopes, a barometer, and a magnetometer. MAVLink is a serial protocol that is the primary means of transmitting sensor data **[21]**. ArduPilot adapts its telemetry rates

using MAVLink Radio.

In advance, we put the deck containers (white color in **Figure 5a**), which are made of Styrofoam and Formax, on the hull. Then we checked the trim, draft, heeling, waterproof conditions, and actuation of the rudder and propeller in an indoor water tank. Because the leads were laid on the bottom of the hull and inside the deck containers, the stability of the VLCS model could not be better. This point is far from reality. The draft, trim, and heel must be trimmed to the cargoes, ballast, and bunkers. The deck containers were fixed to prevent collapse. One can see the single box of autonomous systems in the middle of the deck containers (**Figure 5b**). The edge of the transom touches the still water surface. The VLCS model was prepared at last.

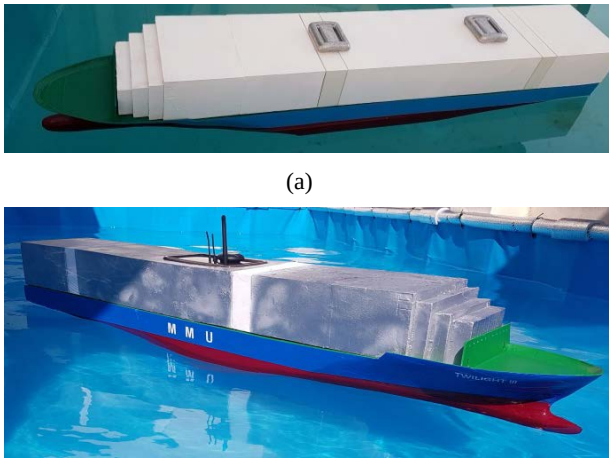

(a)

(b)

Figure 5: The tests of heeling, trim, and waterproof conditions

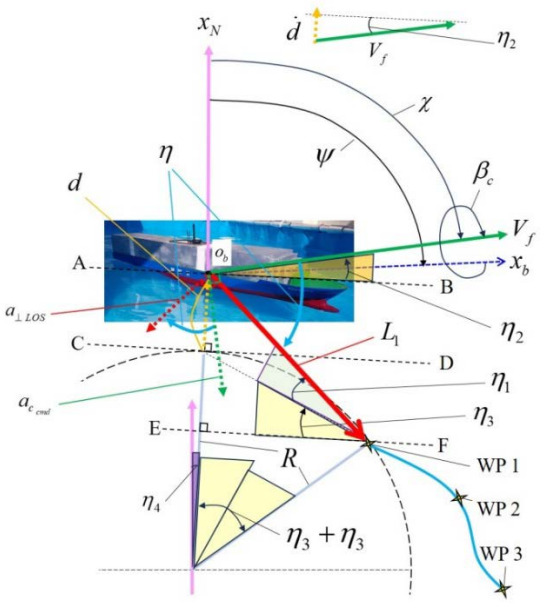

Figure 6: Guidance law

2.2 Guidance law

The guidance law in ArduPilot originated from the principles of an Unmanned Aerial Vehicle (UAV) system **[22]**. We illustrated the marine situation of autonomous tracking tasks in **Figure 6**. The container ship has a position of course track errors (d). The center of the frame (o_b) is fixed on the center of gravity (CG). The local position may have the cross-track errors from the tangential line ($\overline{CD}$), which is parallel to the lines of $\overline{AB} \parallel \overline{EF}$.

The model is on a North-East-Down (NED) frame, where the north axis is directed to the true north (x_N). The pink lines mean the same direction. The yaw angle (ψ) is from the x_N to the direction of x_b axis. The ship plans to navigate to the next waypoint (WP) 1 autonomously. The red thick line means the well-known L_1 distance (See **Table 2**), which is denoted as:

$$L_1 = \frac{1}{\pi} D_{L1} \cdot T_{L1} \cdot V_f \tag{1}$$

where D_{L1} is the damping, named as *NAVL1_DAMPING* in the ArduPilot; T_{L1} is the period, which is one key parameter, as named *NAVL1_PERIOD*; V_f is the forward speed (See **Table 2**) **[23]**. The η denotes the angle between the V_f and L_1 distance. This angle is the same as the sum of η_1, η_2, and η_3. According to the definition of radian, the arc length (s) is $R\eta$, where R is the radius of circle; η is in radians. The maximum distance from a WP is denoted as *WP_RADIUS* **[23]**. We can assume such that $\eta_1 \approx d/L_1$ and $\eta_2 \approx \dot{d}/V_f$. When the USV is controlled to reach the WP 1, the yaw angle (ψ) is adjusted, of course, as with the existing marine vessels. There may be ocean disturbances, so the actual direction normally can be varied as the course angle (χ). Both the angles (ψ, χ) are measured as the clockwise direction from the x-axis (x_N), which indicates the true north. The crab angle (β_c) is not very important in the study. We can see the two dashed lines in **Figure 6**, where $a_{\perp LOS}$ denotes the acceleration perpendicular to the L_1; $a_{c_{cmd}}$ means the lateral (centripetal) acceleration command, which is calculated by the PD controller

Table 2: Main parameters of the L_1 Controller

Parameters	Values	Unit
NAVL1_DIST	3	m
NAVL1_PERIOD	15	s
NAVL1_DAMPING	0.75	-
WP_RADIUS	2	m

such that:

$$\alpha_{c_{cmd}} = k_d\dot{d} + k_s d + \frac{V_f^2}{R}, k_s = 1/T_{L1}^2 \quad (2)$$

where $k_d, k_s(>0)$ are the damping and restoring constants, respectively **[24]**. The key parameters of the L_1 controller are listed in **Table 2**.

In addition, the $\alpha_{s_{cmd}}$ is approximately equal to $-\ddot{d}$, a second-order Ordinary Differential Equation (ODE) of course track errors can be calculated as:

$$\ddot{d} + 2\zeta\omega_n\dot{d} + \omega_n^2 d \approx 0 \quad (3)$$

with $\omega_n = \sqrt{\frac{k_x}{m}} = \sqrt{2}Vc/L_1, c \equiv cos\,\eta_3$, and

$\zeta = \frac{k_d}{2\sqrt{mk_s}} = \frac{1}{\sqrt{2}} = 0.707,$

where ζ is the small damping coefficient; ω_n is the natural frequency of a resonator (rad/s), which is dependent on the speed and the L_1 distance, like the concept of Line of sight (LOS); $m$is the mass (11,480 g) of the typical Mass-Damper-Spring system.

3. Experimental Tests

3.1 Experimental place

Actually, we did not perform the collision avoidance, zig-zag test, berthing, or unberthing in this time, rather, focus on course-keeping ability, the lower vibrations, and rotational stability at sea. **Figure 7** shows the place of test. Yeosu City is one of the marine cities in South Korea. The test date was 1 March, 2025. This coastal sea looks so clear; however, it represents dynamic scenes whenever we test. There are tourists on the beach and rocks at close distances. Sometimes we have to encounter low tides, seaweed, aquatic plants, and fishing nets. More interestingly, divers are working on the spot because it is the coast of a fishing village. After the rainy season, large amounts of waste from the town and the mountain prevent the test because of concerns about the damage to actuators. Outside of the yellow line, frequent traffic or berthing ships exist. Can we establish these things in each simulation?

Figure 7: Experimental place: Yeosu, S. Korea

Table 3: Information on the wave

Parameters	0600 LT	0700 LT
Maximum wave height	0.7 m	0.6 m
Significant wave height	0.5 m	0.4 m
Average wave height	0.3 m	0.2 m
Wave period	6.4 sec	5.8 sec

Table 4: Information on the wind speed

Parameters	Yeosu	Unit
Average wind speed	2.3	m/s
Maximum wind speed	4.8	m/s
Direction of maximum wind speed	70	deg
Maximum instantaneous wind speed	6.9	m/s
Direction of maximum instantaneous wind speed	90	deg
Time of maximum instantaneous wind speed	06:46	
Time of maximum wind speed	06:49	

Information on waves and winds is listed in **Tables 3** and **4**, where taken from the National Climate Data Center **[25]**. The nearest official data on the wave of 1 March, 2025, is observed at the Nam-Hae in South Korea 26km off from the test place. Because the beach of experiment is closer to the Yeosu city, the wave height is less than that in **Table 3**. We started the tests in the mornings between 0600 and 0800 Local Time (LT). The wind speed was weak. We can see that the maximum wind speed and directions of air flow are from the sea.

3.2 Results of trajectories with waypoints

Figure 8 shows the snapshots of routes on the Mission Planner (MP) screen. The red line shows the results of the trajectories. We introduced this one result in the study, considering the number of test results. The corner of the right-down explicitly stated the date of the test. Our scenario is the star-shaped routes because we want to see the course track errors and performance after arriving at the WPs and the sharp turning of the USV. The advantage of the USV systems is that the results show a constant pattern. It cannot get out of its performance. By humans, one may mistake their duty watch because of many human factors.

The course track errors, which were explained in the previous

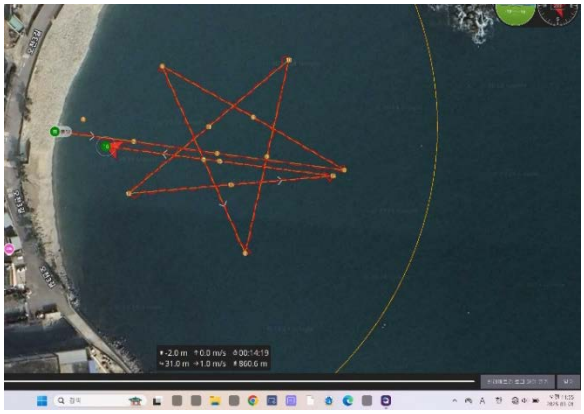

Figure 8: trajectories on the Mission Planner

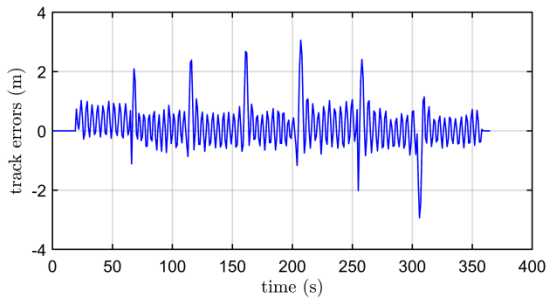

Figure 9: track errors

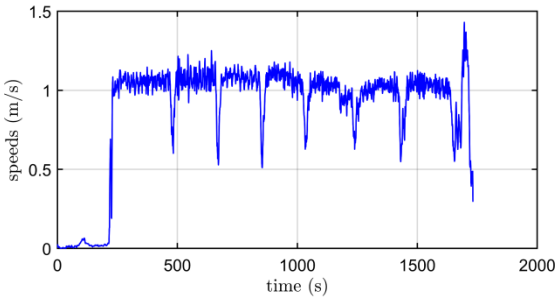

Figure 10: speeds

section, are illustrated in **Figure 9**. Over 2 m results are the 6 edges of routes in **Figure 8**. The remaining courses are recorded with an error of less than 1 m. This model features a single rudder, allowing the ship to navigate with a slight zig-zag motion. On that day, there are no terrible wind gusts and rough waves. Of course, only the surface wave will be a burden on this size of model.

Although the sea test, the model shows a certain level of speed (**Figure 10**). We set the speed to 1 m/s with a Froude number (*Fn*, $U/\sqrt{gL}$) of 0.286. The design speed of a container ship and *Fn* are 24 to 26 knots and 0.22 to 0.25 **[26]**, respectively. Thus, the actual speed of 0.8 m/s is more appropriate considering surge resistance. This cannot be changed during the navigation. It is a different point with a car driving. When we drive the car at a steep curve on the road, the speed can decline by deceleration. This model cannot be changed in its speed. Only the rudder action controls the position of the ship. So, we said that the yaw angle of the guidance law is one of the important keys. The result of a constant level of speed means that the ship overcomes the wave resistance. About half of the speed decreased at the six edges. The final peak of results was not the route. At that time, we recovered the ship from the sea. Then we have to check the ship's condition.

The WPs and trajectories are compared in **Figure 11**. Red circles are WPs on the MP screen. Green dashed lines are connections between the WPs. The ship started west of **Figure 11**. It goes to the east side of the map, then comes back to the start position after navigating with a star-shaped route. Because the ship has a constant speed, it deviates at the edges of the routes. We think about the speed reduction of the corners in future tests.

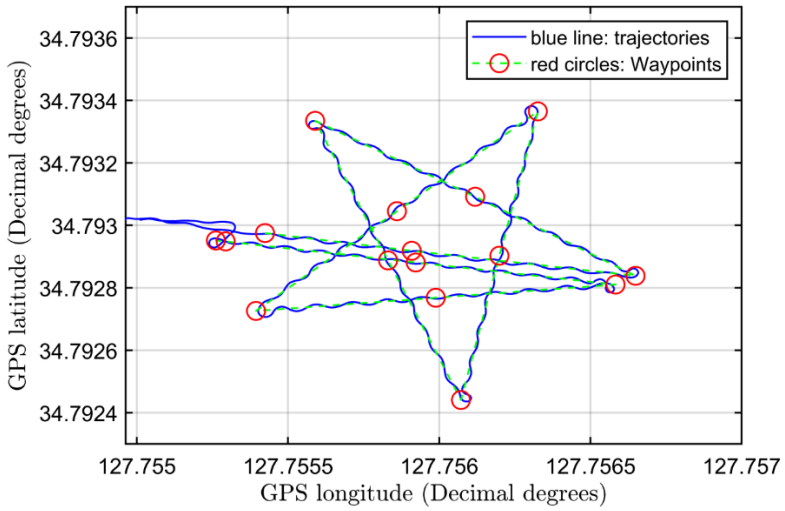

Figure 11: Waypoints (WPs) and results of trajectories

Table 5: Results of rotational responses

Parameters	Roll angle (degree)	Pitch angle (degree)
Maximum angle	-18.8	-3.3
Mean (average)	-1.72	-0.10
Standard deviation	52.97	3.11

3.3 Results of roll, pitch, and yaw responses

In this section, the responses of the main states are represented. The roll motions (**Figures 12, 13)** are one of the important considerations. **Table 5** presents the basic statistical results of the rotational responses, with a population of 949. The abnormal values of roll motions are frequent than those of pitch motion, resulting in larger standard deviations compared to the pitch angle.

The concerns of capsizing, we do not have to worry about because the model has a flat-type of bottom and the lead on the inner space of the hull, and the weights of the deck container are not so heavy. This point is far from reality, such that the ability of maximum cargoes is not emphasized in the model. The hull of a container ship is designed in such a form, even though the resonance roll may be anticipated owing to the vertical height of deck containers and high propulsion for achieving the on-time voyages. Roll angles are not exceeded by 10 °, and their rate responses are higher than the roll angle. It means that the ship recovers to an upright position shortly. It has good stability performance in a transversal direction. Pitch responses (**Figures 14, 15**) show no special features. The bow shape of the model cuts through the sea surface very well. Considering the model has a full draft, the pitch responses are not bad. In addition, the rates of pitch are higher than the angles. In some intervals, the pitch rate was varied. This point is not so important because the ship moves while floating on the sea, and the weather conditions. We thought the routes were not straight or circular paths.

Yaw angles and rates (**Figures 16, 18**) recorded the general courses of the ship. We can know the ship's states and the routes from the information on yaw angles only. It did not overstep the 180 °. The headings (**Figure 17**) provide the information by comparison. The actual course angle (χ) of the model is different from these two angles. The forward speed (V_f) does not coincide with the ship's heading. Ocean environments affected the test. That's

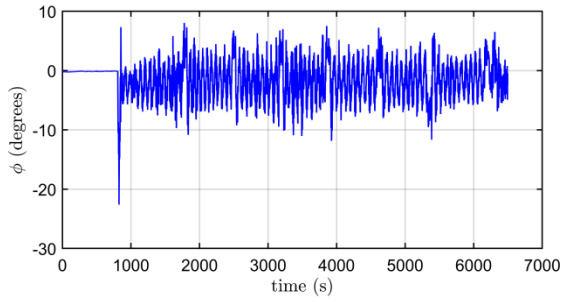

Figure 12: roll responses

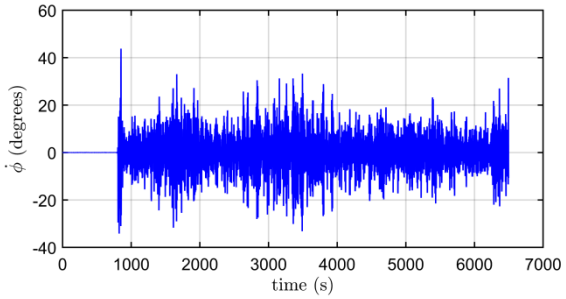

Figure 13: roll rate responses

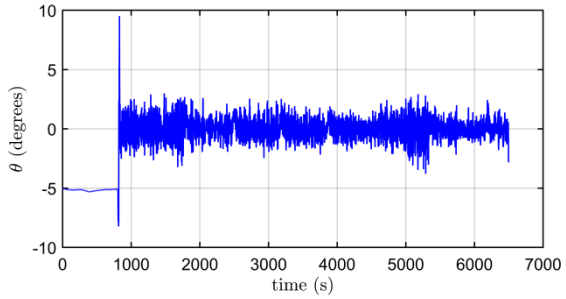

Figure 14: pitch responses

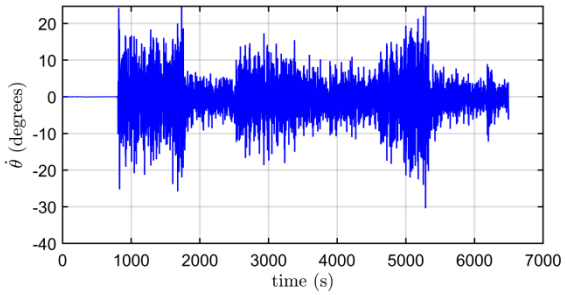

Figure 15: pitch rate responses

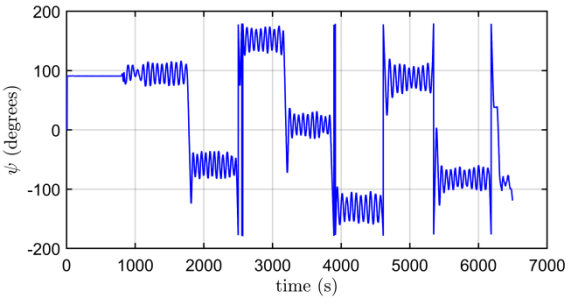

Figure 16: yaw responses

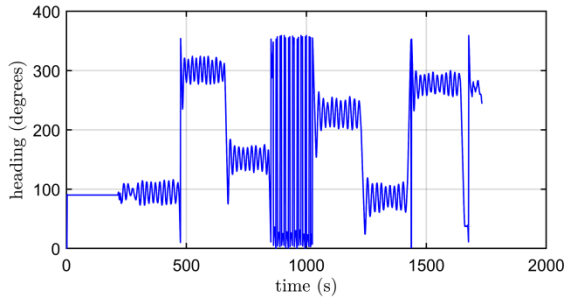

Figure 17: headings

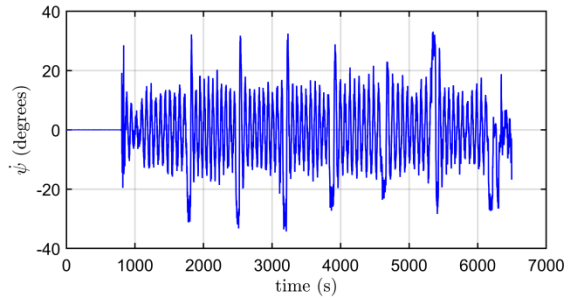

Figure 18: yaw rate responses

why the guidance law and tuning parameters in **Table 2** are necessary.

3.4 Results of Vibrations

The IMU Batch Sampler gathers high-frequency data for spectral analysis from the IMU sensors. Accelerometer data recorded is converted into the frequencies of the vibration **[27]**. The vibrations for each axis resulted in a comparatively low level, especially compared to UAV cases, where the vibrations are acceptable if they represent less than 30 m/s/s. These points are strong for marine vessels when we think about the origin of guidance law and its many UAV users. The wide transom with flat buttock shape helps to reduce resistance and vibrations **[28]**. These results are one of the satisfactory outcomes. Especially, the surge vibrations with low magnitude stipulated to us that the model can navigate the beach.

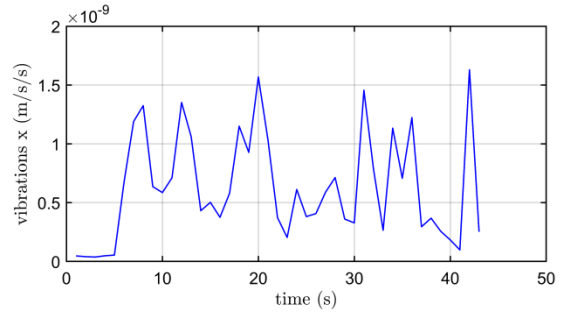

Figure 19: vibrations of the x-axis

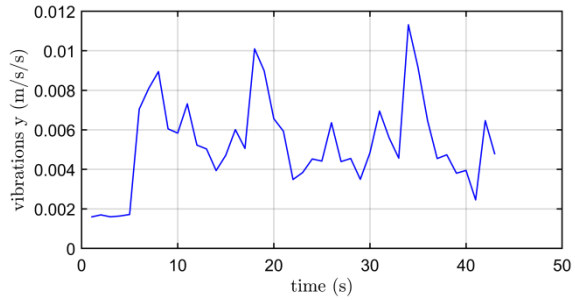

Figure 20: vibrations of the y-axis

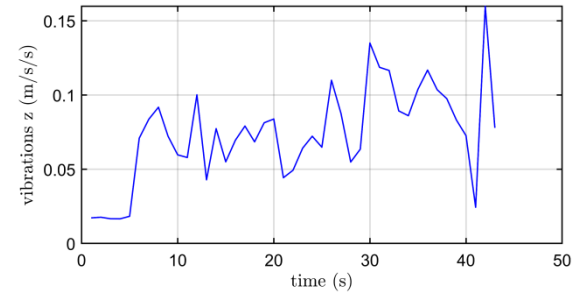

Figure 21: vibrations of the z-axis

4. Conclusion

This study organizes the experiment on the course-keeping ability of a very large container ship model. We focused on the course track errors, vibrations, and rotational responses during autonomous test. We obtained the following results and problems of a container ship model.

1) The course track errors were recorded with an error of less than 1 m except over 2 m in the edges of a star-shaped route.
2) The desired speed is not much decreased during the test. It is far from reality because the weight of the deck container is not so heavy. 'Viscous resistance' will be the next topic of importance.
3) The bow shape of the model cuts through the sea surface effectively, as evidenced by the vibration in the x-direction that does not exceed 1.5×10^{-9} m/s/s.
4) The roll angles were not exceeded by 10 ° during autonomous course-keeping test.
5) The performances of rotational responses, vibrations, and seaworthiness were difficult to resemble the real ships because the multi-functionalities of the vessels were limited. That's why most experiments with model ships are difficult to match real ships.
6) The fiberglass materials and the 1.2m LOA were unsatisfactory to the authors because it is not fully strong and the

length falls short of the general human height as well. In the next work, the author will advance the longitudinal length and the structural frames. Steel hull will be considered in future studies.

7) As our original goal of enhancing the course-keeping ability with PD control has been achieved, we can suggest that the Pixhawk 4 and QGroundControl can be effective to the marine vehicles. Our model of fiberglass material can be recommended, unlike **[16]**. We have applied to the marine vessel and it seem not so complicated to organize the experimentation personally until this stage.

The model experiments remain limited and stimulate the next challenges in many ways. However, a cut-down test is useful to tackle the inherent problems and safety of autonomous ships in the marine industry. To the best of the author's knowledge, the model experiments are still necessary even though they involve many disagreements and simplifications. Considering the above problems, the author is adjusting the length or construction of the model ship to be as close to the human for future studies.

Author Contributions

Conceptualization, S. D. Lee; Methodology, S. D. Lee; Software, S. D. Lee; Formal Analysis, S. D. Lee; Investigation, G. S. Jeong; Resources, G. S. Jeong; Data Curation, G. S. Jeong; Writing-Original Draft Preparation,G. S. Jeong; Writing-Review & Editing, S. D. Lee; Visualization, S. D. Lee; Supervision, S. D. Lee.

References

[1] M. Faraday, "On a peculiar class of acoustical figures; and on certain forms assumed by groups of particles upon vibrating elastic surfaces," Philosophical Transactions of the Royal Society of London, vol. 121, pp. 299-340, 1831.

[2] S. D. Lee, S. S. You, L.N.B. Long, B. D. H. Phuc, and H. S. Kim, "Active control synthesis for parametric instability of container ship model", Acta Mechanica, vol. 235, pp. 5673-5696, 2024.

[3] Wikipedia, 2025. List of largest container ships, Wikimedia Foundation, Inc., https://en.wikipedia.org/wiki/List_of_largest_container_ships, Accessed August 2, 2025.

[4] The Society of Naval Architects of Korea, Closing Ceremony of the 5th Autonomous Boat Competition 2024, https://www.youtube.com/watch?v=LQ3MkRTiTww, Accessed August 22, 2025.

[5] G. S. Jeong, S. J. Lee, and S. D. Lee, "Autonomous surveillance maneuvers for marine vessels in specially designated waters with a focus on the consecutive port and starboard turning cases", Journal of Advanced Marine Engineering and Technology, vol. 46, no. 5, pp. 237-247, 2022.

[6] NIFS, Announcement of cost calculation criteria for use of fisheries engineering tanks, National Institute of Fisheries Science, 2022.

[7] S. J. Ahn, M. C. Won, S. Y. Kim, and H. S. Park, "Joystick control algorithm for berthing and unberthing of waterjet propelled unmanned surface vehicle using actuator nonlinear model," Journal of the Society of Naval Architects of Korea, vol. 60, no.3, pp 165-174, 2023.

[8] R. Pasini, Researchers use CFD for path-following performance of autonomous ships, WTWH Media (Engineering), LLC, 2024. https://www.engineering.com/researchers-use-cfd-for-path-following-performance-of-autonomous-ships/, Accessed August 23, 2025.

[9] Y. K. Kwak, "Viscous resistance analysis of a ship using numerical solutions," Journal of Ocean Engineering and Technology, vol. 11, no. 2, pp. 100–106, 1997 (in Korean).

[10] G. Cao, Z. Jia, D. Wu, Z. Li, W. Zhang, "Trajectory tracking control for marine vessels with error constraints: A barrier function sliding mode approach", Ocean Engineering, vol. 297, 116879, 2024.

[11] G. Chen, Y. Li, H. Zike, S. Yang, "Autonomous navigation algorithm for underactuated unmanned surface vehicle based on model predictive control," Journal of Shanghai Jiaotong University, 2023.

[12] V. Sonntag, A. Perrusquía, A. Tsourdos, and W. Guo, "COLREGs compliance reinforcement learning approach for USV maneuvering in track-following and collision avoidance problems," Ocean Engineering, vol. 316, 119907, 2025.

[13] L. Zhang, S. Zhang, Z. Du, H. Li, L. Gan, and X. Li, "Adaptive trajectory tracking of the unmanned surface vessel based on improved AC-MPC method", Ocean Engineering, vol. 322, 120455, 2025.

[14] C. Wu, W. Yu, W. Liao, and Y. Ou, "Deep reinforcement learning with intrinsic curiosity module-based trajectory tracking control for USV," Ocean Engineering, vol. 308, 118342, 2024.

[15] X. Liu and W. Zhang, "Prescribed performance actuator-tolerance control for path following of unmanned surface

vessels via the triggered adaptive line-of-sight guidance," Computers and Electrical Engineering, vol. 120, Part A, 109617, 2024.

[16] B. S. Kang and C. H. Jung, "A study on automatic operation control of autonomous ships", Journal of the Korean Society of Marine Environment and Safety, vol. 27. no. 1, pp. 38-46, 2021.

[17] QGroundControl, Drone Control, 2019. Available: https://qgroundcontrol.com/, Accessed August 2, 2025.

[18] MathWorks, PX4 Autopilot in Hardware-in-the-Loop (HITL) Simulation with UAV Dynamics in Simulink, 2025. https://se.mathworks.com/help/uav/px4/ref/hitl-simulink-plant-example.html, Accessed August 23, 2025.

[19] DNV, Vessel register for DNV, 2022. Available: https://vesselregister.dnv.com/vesselregister, Accessed August 2, 2025.

[20] ARDUPILOT, Measuring Vibration with IMU Batch sampler, ArduPilot Dev Team, 2024.

[21] ARDUPILOT, MAVLink Basics, ArduPilot Dev Team, 2024.

[22] S. H. Park, J. Deyst, and J. P. How, "A new nonlinear guidance logic for trajectory tracking", Proceedings of the AIAA Guidance, Navigation and Control Conference and Exhibit, Aug 2004, Providence, Rhode Island, 2004.

[23] ArduPilot, ARDUPILOT Versatile, Trusted, Open: Navigation Tuning, ArduPilot Dev Team, 2024.

[24] M. S. Grewal and A. P. Andrews, Kalman Filtering, Theory and Practice using Matlab, 3rd Edition: John Wiley & Sons, Inc., pp. 51-52, 2008.

[25] KMA, Climate Statistics Analysis, National Climate Data Center, https://data.kma.go.kr/climate/RankState/selectRankStatisticsDivisionList.do?pgmNo=179, Accessed August 23, 2025.

[26] The Society of Naval Architects of Korea, Ship Resistance and Propulsion, pp. 173-178, 2009.

[27] ARDUPILOT, Measuring Vibration with IMU Batch sampler, ArduPilot Dev Team, 2024.

[28] L. Larsson and H. C. Raven, "Ship resistance and flow, Principles of naval architecture series", The Society of Naval Architects and Marine Engineers, 601 Pavonia Avenue, Jersey City, NJ 07306, pp. 166-214, 2010.